A Novel High-Sensitivity Broadband Rectifier for Ambient RF Energy Harvesting

Xuehua WANG [1], Baokun JIN [2], Lichang HUANG [2], Man ZHANG [2], Ming FANG [1]

[1]Jianghuai College of Anhui University, Hefei 230031, China
[2] Key Lab of Ministry of Education of Intelligent Computing & Signal Processing, Anhui University, Hefei 230601

jhxywxh@126.com

Submitted August 3, 2021 / Accepted June 22, 2022 / Online first July 15, 2022

Abstract. *In this paper, a novel high-sensitivity broadband rectifier is proposed aiming at ambient radio frequency (RF) energy harvesting. Traditionally, voltage doubling rectifying circuit is used to design high-sensitivity rectifier. But when the input power is lower, the rectifying efficiency is significantly reduced. Therefore, an improved parallel half-wave rectifying circuit is proposed in this article which can convert RF energy in the whole period. And the proposed rectifying circuit can work better in lower power environment and has a higher efficiency level. Besides, the impedance match is also important component of rectifier. Due to the nonlinearity and complexity of rectifying circuit, achieving wideband matching network is a challenge. Thus, a design approach of broadband impedance circuit is given in this study. Combining with the proposed high-sensitivity rectifying circuit, a high-sensitivity wideband rectifier can be generated, when the input power is –15 dBm, –20 dBm, –25 dBm, the efficiency is 43%, 32%, 20%, respectively. Finally, a second-order wideband rectifier with high sensitivity is realized, and the range of bandwidth can cover four main frequency bands of GSM 900 MHz, GSM 1800 MHz, UMTS 2100 MHz, WLAN 2400 MHz. To verify the validity, the rectifier is fabricated and measured, and the measurement has a good agreement with simulation results.*

Keywords

High-sensitivity, broadband rectifier, RF energy harvesting

1. Introduction

As the development of Internet, there are existing many wireless sensor nodes around environment. How to supply power to these sensor nodes, is the main problem facing now. Traditionally, the battery is regarded as power supply for nodes, but the operating cost of this method is much higher and it is not convenient to replace the battery in some dangerous or remote place. As the rapid growth of communication industry, the RF energy around environment gets more and more rich. For example, there are all kinds of wireless signal transmitting devices, such as mobile phone base stations, TV towers, wireless routers and so on. In addition, the progress of semiconductor technology is also a contribution that the RF energy harvesting technology becomes the self-powered solution of Internet of Things, which can satisfy the power supply of low-powered equipment. On account of the technology has advantages of stability and non-pollution, it is concerned by many researchers recently.

Because of the RF energy around environment is feeble, it is crucial for rectifier to have a high sensitivity. Meanwhile, wide impedance bandwidth is required in order to harvest more energy. To survey the distribution of RF energy, usually, the means combining spectrum analyzer with wide-band horn antenna is adopted. The study shows that there are four main frequency bands in environment which have higher power energy density, corresponding to 800–960 MHz, 1790–1880 MHz, 2100–2170 MHz, 2380–2450 MHz, respectively [1–3]. At present, there are three primary forms: single-band, multiband and wideband rectifier. For single-band rectifier [4–8], although it has higher efficiency, only the energy of a single band can be collected. Besides, several rectifying branches and antennas are designed to harvest the energy of the respective frequency band, which can also harvest several target-band energy. In [1], four rectennas are designed to harvest the energy of DTV, GSM 900, GSM 1800 and 3G, but this way has even larger size of circuit. About multiband rectifier [9–14], it can harvest the energy of multiple target bands by designing multiband impedance matching circuit. In [9], a multi-stub matching circuit is introduced to design a dual-band rectifier operating at 2.1 GHz and 2.45 GHz, but the efficiency is lower when the input power is feeble. In [10], a quad-band rectifier is realized by paralleling four branches, which can operate at GSM 900, GSM 1800, UMTS 2100 and WiFi. In [11], using the same approach, a multi-band rectifier circuit composed of four single-loop rectifiers can obtain high conversion efficiency. In [12], a new tri-band power rectifier was proposed with an efficiency of more than 46.5% at 0 dBm input power, but lower input power was not considered. In [13], a novel six-band dual circular polarization rectenna for ambient RF

DOI: 10.13164/re.2022.0331

energy harvesting is generated, and the six-band rectifier is achieved by using improved impedance matching circuit with three paralleling branches. But the efficiency is still lower. As for wideband rectifier [14–19], it can harvest more energy in a wide range of frequency band, but it is always challenging. In [16], a novel ultrawideband rectenna is presented by using hybrid resistance compression technology to improve the impedance matching performance over a wide frequency range, which has high rectifying efficiency from 450 MHz to 900 MHz. In [17], an impedance matching network with additional quarter wavelength shorting was designed to achieve broadband impedance matching of the rectifier. The efficiency is above 50% when the input power is in the range of 3–15 dBm. In [18], a new broadband rectenna for ambient energy harvesting is realized, and a novel two-branch impedance matching circuit is introduced to enhance the characteristic of bandwidth and efficiency. When the input power is –10 dBm, the efficiency can reach 55%. But the rectifying efficiency is still a little lower at a relatively lower ambient input power level.

Therefore, this paper presents an improved parallel half-wave rectifying circuit which has higher rectifying efficiency at lower input power level. Basing on the proposed high-sensitivity rectifying circuit, a design method of broadband impedance circuit is also presented. In conclusion, a high-sensitivity broadband rectifier can be achieved by combining the high-sensitivity rectifying circuit with wideband impedance matching circuit. Firstly, this article generates a high-sensitivity broadband rectifier operating form 1.9 GHz to 2.5 GHz. Then, a dual-band rectifier working at GSM 900 and GSM 1800 is introduced. Finally, basing on the above two rectifiers, a new rectifier topology is proposed, which can cover four major frequency bands of GSM 900 MHz, GSM 1800 MHz, UMTS 2100 MHz and WLAN 2400 MHz.

2. Rectifier Design and Analysis

2.1 High-Sensitivity Rectifying Circuit

Usually, the voltage doubling rectifying circuit is utilized to design high-sensitivity rectifier at low input power level. But the rectifying efficiency is not enough for ambient RF energy harvesting, hence, this paper proposes an improved parallel half-wave rectifying circuit which has higher efficiency under low power. The rectifying circuit is presented in Fig. 1.

In Fig. 1(a), the improved rectifying circuit consists of series inductance L0, shunt capacitor C0, shunt diode D1 (SMS 7630-079) and series capacitor C1. The load resistance is chosen as 2700 Ω, L_0 = 10.7 nH, C_0 = 1000 nF, C_1 = 520 nF. Z1 and Z2 are the input impedance from A to Path 1 and Path 2, respectively. Comparing with voltage doubling rectifying circuit, the improved rectifying circuit uses one diode only, which consumes lesser energy when the input power is lower. The fundamental theory is as follows:

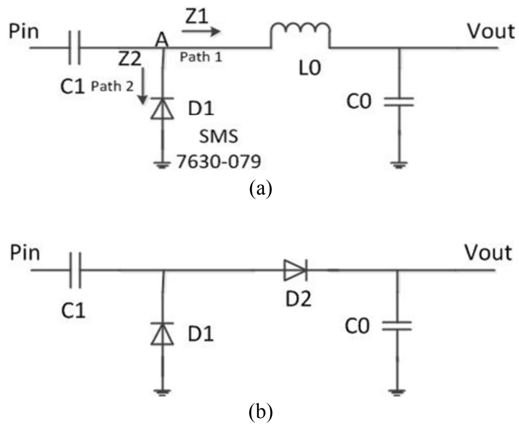

Fig. 1. (a) Improved rectifying circuit. (b) Voltage doubling rectifying circuit.

When the first positive half period of signal comes, the diode D1 is cut-off, the signal reaches the Vout port through Path 1. When the first minus half period comes, the diode is turn on. Because the impedance value from A to Path 1 is more than the impedance value from A to Path 2, the signal is preferring to getting through Path 2, and the energy is stored in capacitor C1. When the second positive half period comes, the diode is cut-off, the energy lying in the first minus half period and the second positive half period reaches the Vout port together through Path 1. In a word, the improved rectifying circuit can also operate at the whole period. Table 1 demonstrates the impedance value of Z1 and Z2 when the input power is –20 dBm.

In order to verify this idea, an improved rectifying circuit and a voltage doubling rectifying circuit are designed, and the comparing result is given in Fig. 2 at –20 dBm input power level.

In Fig. 2, the result shows that the return losses between voltage doubling and improved rectifying circuit are nearly same, and even the return loss of voltage doubler is even better comparing with the improved rectifying circuit, but the efficiency of improved rectifying circuit is much higher than voltage doubler. Hence, the improved rectifying circuit has higher efficiency at a low ambient power level.

f (GHz)	Z1	Z2
1.8	1.258E3/–82.341	77.144/–42.252
1.9	681.733/–85.440	73.482/–27.490
2.0	467.785/–86.495	76.264/–13.325
2.1	355.061/–86.960	83.806/–1.571
2.2	284.511/–87.152	96.035/7.362
2.3	235.369/–87.171	114.105/13.618
2.4	198.394/–87.042	139.163/16.974
2.5	168.772/–86.747	173.683/17.134

Tab. 1. The Z1 and Z2 change with frequency (unit: Ω).

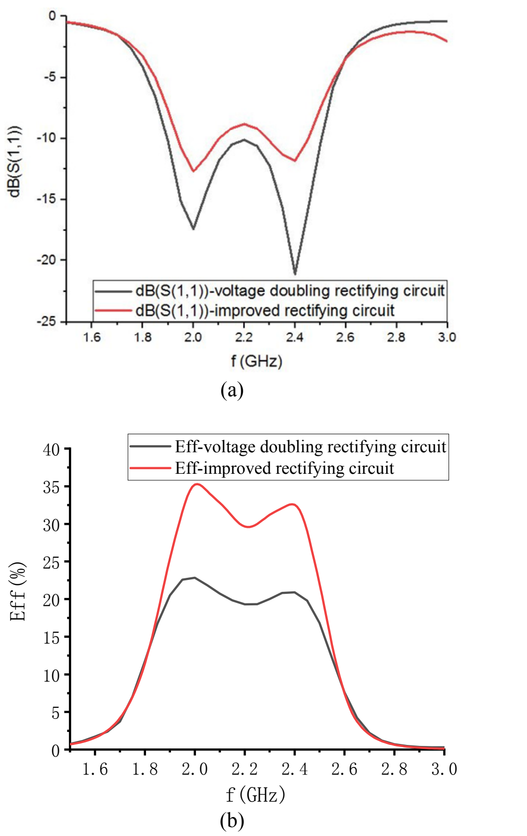

Fig. 2. (a) The reflection coefficient comparison. (b) The efficiency comparison.

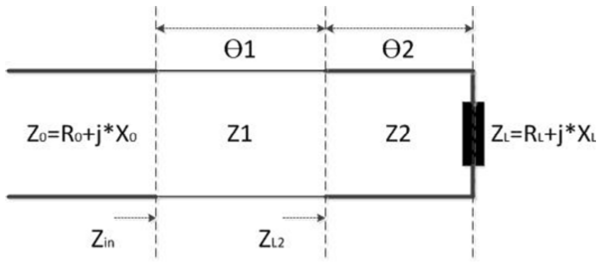

Fig. 3. Second order dual-frequency matching for complex impedances

2.2 Wideband Impedance Matching Circuit

Due to the nonlinearity and complexity of the rectifying circuit, an impedance matching circuit is required to connect the front-end antenna with back-end rectifying circuit. In this text, a design method of wideband impedance matching circuit is introduced, and combining with the above high-sensitivity rectifying circuit, a novel high-sensitivity broadband rectifier can be achieved. Firstly, a second order dual-frequency matching technology for complex impedances is introduced [20], and the structure diagram is displayed in Fig. 3 where Z1 and Z2 are the characteristic impedance, θ1 and θ2 are electrical length, Z0 is source impedance, ZL is load impedance, Zin and ZL2 are input impedance.

According to the theory of transmission line, the input impedance can be expressed:

$$Z_{\mathrm{in}} = Z_1 \frac{Z_{\mathrm{L2}} + \mathrm{j}Z_1 \tan(\theta_1)}{Z_1 + \mathrm{j}Z_{\mathrm{L2}} \tan(\theta_1)}, \tag{1}$$

$$Z_{\mathrm{L2}} = Z_2 \frac{Z_{\mathrm{L}} + \mathrm{j}Z_2 \tan(\theta_2)}{Z_2 + \mathrm{j}Z_{\mathrm{L}} \tan(\theta_2)}. \tag{2}$$

In order to maximize the transfer of energy, a conjugacy relation can be written:

$$Z_{\mathrm{in}} = Z_0^* = R_0 - \mathrm{j}X_0\,. \tag{3}$$

Combining with (3), equation (1) can be written as:

$$Z_{\mathrm{L2}} = Z_1 \frac{R_0 - \mathrm{j}X_0 - \mathrm{j}Z_1 \tan(\theta_1)}{Z_1 - X_0 \tan(\theta_1) - \mathrm{j}R_0 \tan(\theta_1)}. \tag{4}$$

Because $Z_{\mathrm{L}} = R_{\mathrm{L}} + \mathrm{j}X_{\mathrm{L}}$, combining equation (2) with (4):

$$Z_2 \frac{R_1 + \mathrm{j}X_1 + \mathrm{j}Z_2 \tan(\theta_2)}{Z_2 + \mathrm{j}(R_1 + \mathrm{j}X_1)\tan(\theta_2)} = Z_1 \frac{R_0 - \mathrm{j}X_0 - \mathrm{j}Z_1 \tan(\theta_1)}{Z_1 - \mathrm{j}(R_0 - \mathrm{j}X_0)\tan(\theta_1)}. \tag{5}$$

Expanding equation (5) and separating the real part and imaginary part:

$$\begin{aligned}&\left(R_{\mathrm{L}}Z_1{}^2 - R_0Z_2{}^2\right)\tan(\theta_1)\tan(\theta_2) = Z_1Z_2(R_{\mathrm{L}} - R_0) + \\ &[Z_1\tan(\theta_2) + Z_2\tan(\theta_1)] \times (R_0X_{\mathrm{L}} - R_{\mathrm{L}}X_0),\end{aligned} \tag{6.a}$$

$$\begin{aligned}&\left(R_0R_{\mathrm{L}} + X_0X_{\mathrm{L}}\right)\left[Z_1\tan(\theta_2) + Z_2\tan(\theta_1)\right] - \\ &Z_2Z_1^2\tan(\theta_1) - Z_1Z_2^2\tan(\theta_2) = \\ &Z_1Z_2\left(X_{\mathrm{L}} + X_0\right) - \left(X_{\mathrm{L}}Z_1^2 + X_0Z_2^2\right)\tan(\theta_1)\tan(\theta_2).\end{aligned} \tag{6.b}$$

To meet equation (6) at f_1 and f_2, the following equations can be obtained where the l_1 and l_2 are the physical length of microstrip line Z1 and Z2, $f_2 = mf_1$, $m > 1$, $\beta = 2\pi/\lambda_1$.

$$\begin{aligned}&\left(R_{\mathrm{L}}Z_1^2 - R_0Z_2^2\right)\tan(\beta l_1)\tan(\beta l_2) = Z_1Z_2\left(R_{\mathrm{L}} - R_0\right) + \\ &\left[Z_1\tan(\beta l_2) + Z_2\tan(\beta l_1)\right]\left(R_0X_{\mathrm{L}} - R_{\mathrm{L}}X_0\right),\end{aligned} \tag{7.a}$$

$$\begin{aligned}&\left(R_0R_{\mathrm{L}} + X_0X_{\mathrm{L}}\right)\left[Z_1\tan(\beta l_2) + Z_2\tan(\beta l_1)\right] - \\ &Z_2Z_1^2\tan(\beta l_1) - Z_1Z_2^2\tan(\beta l_2) = \\ &Z_1Z_2\left(X_{\mathrm{L}} + X_0\right) - \left(X_{\mathrm{L}}Z_1^2 + X_0Z_2^2\right)\tan(\beta l_1)\tan(\beta l_2),\end{aligned} \tag{7.b}$$

$$\begin{aligned}&\left(R_{\mathrm{L}}Z_1^2 - R_0Z_2^2\right)\tan(m\beta l_1)\tan(m\beta l_2) = Z_1Z_2\left(R_{\mathrm{L}} - R_0\right) \\ &+\left[Z_1\tan(m\beta l_2) + Z_2\tan(m\beta l_1)\right]\left(R_0X_{\mathrm{L}} - R_{\mathrm{L}}X_0\right),\end{aligned} \tag{7.c}$$

$$\begin{aligned}&\left(R_0R_{\mathrm{L}} + X_0X_{\mathrm{L}}\right)\left[Z_1\tan(m\beta l_2) + Z_2\tan(m\beta l_1)\right] - \\ &Z_2Z_1^2\tan(m\beta l_1) - Z_1Z_2^2\tan(m\beta l_2) = \\ &Z_1Z_2\left(X_{\mathrm{L}} + X_0\right) - \left(X_{\mathrm{L}}Z_1^2 + X_0Z_2^2\right)\tan(m\beta l_1)\tan(m\beta l_2).\end{aligned} \tag{7.d}$$

From (7), we can know that equations have four variables of Z_1, Z_2, βl_1, βl_2, and R_0, R_{L}, X_0, X_{L}, m are known. But equation (7) is nonlinear, it can't get the analytical solution well unless $X_0 = 0$, $X_{\mathrm{L}} = 0$ [19–21]. Of course, an approximate numerical solution can be realized, as follows:

Basing on [21], the initial values can be obtained:

$$l_{1s} = l_{2s} = \frac{\lambda_1}{2(1+m)}, \tag{8.a}$$

$$Z_{1s} = \sqrt{\frac{R_0\left(R_L - R_0\right)}{2\tan^2\left(\frac{\pi}{1+m}\right)} + \sqrt{\left[\frac{R_0\left(R_L - R_0\right)}{2\tan^2\left(\frac{\pi}{1+m}\right)}\right]^2 + R_0^3 R_L}}, \tag{8.b}$$

$$Z_{2s} = \frac{R_L R_0}{Z_{1s}}. \tag{8.c}$$

Supposing Z_{L2} has a conjugate relation between f_1 and f_2:

$$Z_{L2} / f_1 = \mathrm{conj}(Z_{L2} / f_2) = R_{L2} + \mathrm{j}X_{L2}. \tag{9}$$

where the conj(·) is conjugate function.

Combining with (9), the other equations can be deduced from (7). Referring to [22–25], we can obtain:

$$Z_1 = \sqrt{R_0 R_{L2} + \frac{X_0^2 R_{L2} - X_{L2}^2 R_0}{R_0 - R_{L2}}}, \tag{10.a}$$

$$Z_2 = \sqrt{R_L R_{L2} + \frac{X_{L2}^2 R_L - X_L^2 R_{L2}}{R_{L2} - R_L}}, \tag{10.b}$$

$$\begin{aligned} \tan\left(\beta l_1\right) &= \frac{Z_1\left(R_0 - R_{L2}\right)}{R_0 X_{L2} - R_{L2} X_0}, \\ \tan\left(\beta l_2\right) &= \frac{Z_2\left(R_{L2} - R_L\right)}{R_{L2} X_L + R_L X_{L2}}, \end{aligned} \tag{10.c}$$

$$\begin{aligned} \tan\left(m\beta l_1\right) &= \frac{Z_1\left(R_{L2} - R_0\right)}{R_0 X_{L2} + R_{L2} X_0}, \\ \tan\left(m\beta l_2\right) &= \frac{Z_2\left(R_{L2} - R_L\right)}{R_{L2} X_L - R_L X_{L2}}. \end{aligned} \tag{10.d}$$

Considering $Z_1 > 0$, $Z_2 > 0$, equation (10) can be simplified to two nonlinear equations:

$$\begin{aligned} & m\arctan\left[\frac{Z_1\left(R_0 - R_{L2}\right)}{R_0 X_{L2} - R_{L2} X_0}\right] \\ &= \arctan\left[\frac{Z_1\left(R_{L2} - R_0\right)}{R_0 X_{L2} + R_{L2} X_0}\right] + \pi, \end{aligned} \tag{11.a}$$

$$\begin{aligned} & m\arctan\left[\frac{Z_2\left(R_{L2} - R_L\right)}{R_{L2} X_L + R_L X_{L2}}\right] \\ &= \arctan\left[\frac{Z_2\left(R_{L2} - R_L\right)}{R_{L2} X_L - R_L X_{L2}}\right] + \pi \end{aligned} \tag{11.b}$$

where Z_1 and Z_2 can be expressed by R_{L2} and X_{L2}, equations (11) only have two variables. The solution of (11) is similar to (7). Firstly, basing on (8) and (2), the initial values of R_{L2}, X_{L2} can be obtained. Secondly, put the initial values of R_{L2}, X_{L2} into (10), the initial values of Z_1, Z_2 can be gained. Then, put the initial values of Z_1, Z_2 into (11), the values of R_{L2}, X_{L2} can be realized. Finally, combining with (10), we can get the values of Z_1, Z_2, βl_1, βl_2. So far, the microstrip line parameter can be determined.

But the dual-band technology only achieves the impedance match at f_1 and f_2, therefore, optimization and adjustment are required. In this paper, the resonant inductance and impedance translation unit (ITU) are introduced to let the real part of Z_L remain stable and let imaginary part of Z_L remain odd-symmetrical about center frequency f_0 in an expected band, then, a wideband match can be realized by choosing two suitable frequencies of f_1 and f_2. The structure diagram is shown in Fig. 4 where L1 is the resonant inductance, D is the Schottky diode, Z_L is the input impedance of the rectifying circuit.

The resonant inductance is introduced to let the intrinsic resonant frequency of the diode move to low frequency, and choosing suitable inductance value by sweeping parameter. The sweeping results are given in Fig. 5.

From Fig. 5, it is shown that when the inductance value is 51 nH, the real part and imaginary part of Z_L change gently in target bands. Usually, the resonant inductance is transformed into a short stub and there is a relationship as follows [26]:

$$l = \frac{11.81L}{Z_0\sqrt{\varepsilon_r}} \tag{12}$$

where L is the inductance value (unit: nH), and l is the physical length of microstrip line (unit: inch).

The ITU is utilized to make the real part of Z_L remain stable and make the imaginary part of Z_L remain odd-symmetrical about the center frequency. The transformed result is demonstrated in Fig. 6.

In Fig. 6, it is shown that the real part is stable and the imaginary part is odd-symmetrical about 2.2 GHz from 1.8 GHz to 2.6 GHz. Two frequencies of f_1 and f_2 can be chosen, then, a wideband impedance match can be achieved by coupling between passbands.

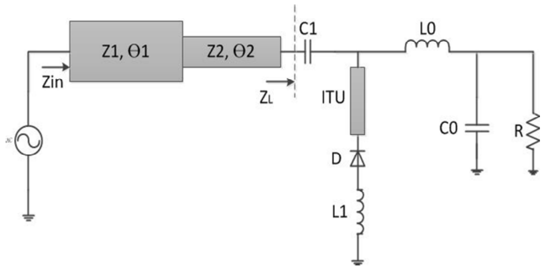

Fig. 4. The topological structure of rectifier.

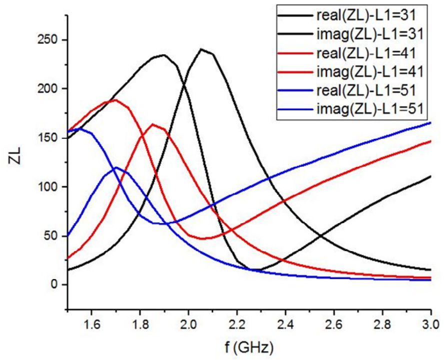

Fig. 5. Sweeping the parameter L1.

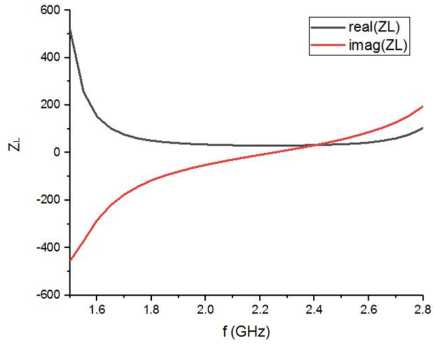

Fig. 6. The real part and imaginary part of Z_L.

2.3 High-Sensitivity Broadband Rectifier

Combining with the above high-sensitivity rectifying circuit and broadband impedance matching circuit, a high-sensitivity broadband rectifier can be achieved. To verify this approach, the high-sensitivity broadband rectifier is simulated and implemented on a 1.575 mm-thick Rogers RO5880 substrate which has a loss tangent of 0.0009 and relative dielectric constant ε_r of 2.2. According to previous section, the parameter values of Z_1, Z_2, βl_1, βl_2 can be calculated as follows:

Firstly, some parameter values can be determined: $f_1 = 2.0$ GHz, $f_2 = 2.4$ GHz, $f_0 = 2.2$ GHz, $m = 2.4/2 = 1.2$, $\lambda_1 = 109.2$ mm. Usually, in front of the rectifier, a receiving antenna is utilized to harvest ambient RF energy, therefore, $Z_0 = 50\ \Omega$, $R_0 = 50$, $X_0 = 0$. The Z_L can be ensured by choosing several impedance points from 1.9 GHz to 2.5 GHz. From Fig. 6, we can know that these impedance values are $40.3 - j\cdot 79$, $34.7 - j\cdot 51.3$, $31.6 - j\cdot 28.7$, $30.6 - j\cdot 9$, $30.9 + j\cdot 10.7$, $31.8 + j\cdot 31.1$, $35.6 + j\cdot 55.8$, respectively, and the average value is $33.6 - j\cdot 10.1$, therefore, $R_L = 33.6$, $X_L = -10.1$.

Combining with (2) and (8), $Z_{L2} = 34.7 + j\cdot 10.6$, the initial values of R_{L2}, X_{L2} are 34.7 and 10.6, respectively. Put the initial values of R_{L2} and X_{L2} into (10), get initial values of Z_1, Z_2: 37, 37.15. Put the initial values of Z_1 and Z_2 into (11), this moment, equations (11) have two variables of R_{L2} and X_{L2}. Theoretically, two equations can solve two variables, but it's difficult to solve R_{L2} and X_{L2} because of the nonlinearity of the equations. In this paper, the solution can be obtained by utilizing the powerful optimization function of MATLAB: $R_{L2} = 40.8$, $X_{L2} = 12.3$. Finally, put the values of R_{L2} and X_{L2} into (10), considering errors and differences, the parameter values can be calculated as: $Z_1 = 34.9\ \Omega$, $Z_2 = 38.7\ \Omega$, $\Theta_1 = 247$ deg, $\Theta_2 = 89.75$ deg.

In a word, the initial parameters of impedance matching circuit can be obtained according to the above calculation. Combining with the proposed high-sensitivity rectifying circuit, a high-sensitivity broadband rectifier is simulated and optimized in Advanced Design System. The final results are given in Fig. 7.

In Fig. 7, when the input power is –20 dBm, the operating bandwidth of rectifier is 1.9 GHz–2.5 GHz and the rectifying efficiency is better than 32%. The layout structure is presented in Fig. 8 and Tab. 2 demonstrates the physical parameter values. Comparing with previous works, the rectifier has higher rectifying efficiency; there is a comparison in Tab. 3.

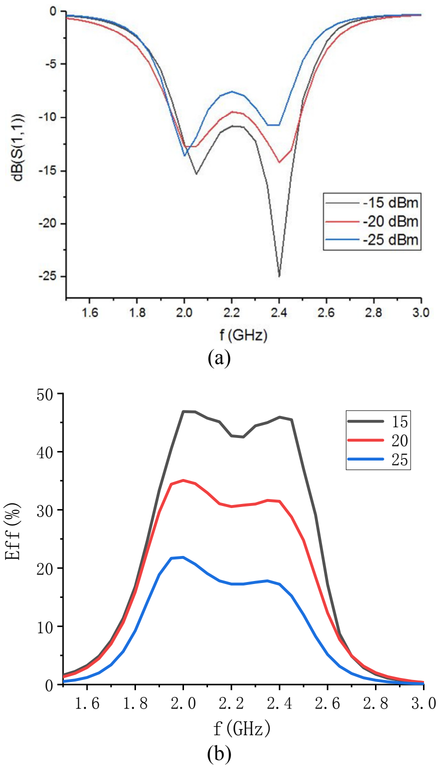

Fig. 7. (a) The reflection coefficient of rectifier. (b) Rectifying efficiency.

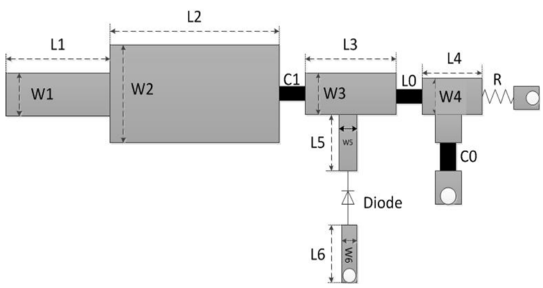

Fig. 8. The layout structure of high-sensitivity broadband rectifier.

L1	W1	L2	W2	L3	W3	L4	W4
12.5	2.5	52.4	6	3.6	5	3	2.3
L5	**W5**	**L6**	**W6**	**L0**	**C0**	**C1**	**R**
16	0.1	14.3	0.1	12 nH	1000 pF	560 pF	2700 Ω

Tab. 2. Physical parameter values of high-sensitivity broadband rectifier (unit: mm).

Ref.	Input power (dBm)	Operating frequency (GHz)	Efficiency
[10]	–15	2.1, 2.45	6%, 16%
[12]	–20	0.55, 0.75, 0.9 1.85, 2.15, 2.45	30%, 28%, 32% 26%, 22%, 20%
[13]	–20	0.915, 1.8	20%, 20%
[16]	–20	1.8–2.5	26%
[17]	–20	0.9, 1.8, 2.05, 2.6	23%, 13%, 11%, 8%
This work	–20	1.9–2.5	32%

Tab. 3. Comparison between the high-sensitivity broadband rectifier and previous works.

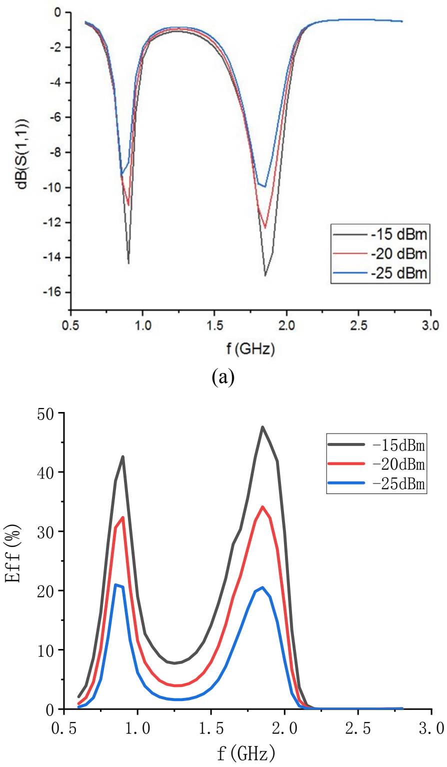

(a)

(b)

Fig. 9. (a) The reflection coefficient of rectifier. (b) Rectifying efficiency.

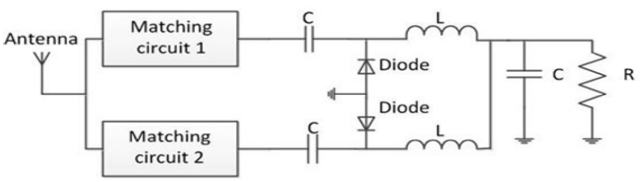

Fig. 10. The topological structure of rectifier.

Basing on Sec. 1, there are four main frequency bands around environment: 800–960 MHz, 1790–1880 MHz, 2100–2170 MHz, 2380–2450 MHz. Because the frequency span of four bands is much larger, it is unpractical to design a rectifier operating at 800–2450 MHz. In order to get more energy, this article designs a parallel impedance matching network, and the upper half part is used to harvest the RF energy of 800–960 MHz and 1790–1880 MHz, the lower half part is utilized to harvest the energy of 2100–2170 MHz and 2380–2450 MHz. The impedance matching network of lower half part can use the above matching circuit of 1.9–2.5 GHz, therefore, an impedance matching circuit working at 800–960 MHz and 1790–1880 MHz is required. According to the dual-band matching technology, a dual-band rectifier operating at 900 MHz and 1800 MHz is designed. The design process is similar to the aforementioned rectifier, and the design results are given in Fig. 9.

In Fig. 9, it's shown that when the input power is –20 dBm, the rectifier operates at 900 MHz and 1800 MHz, and the efficiency is better than 32%.

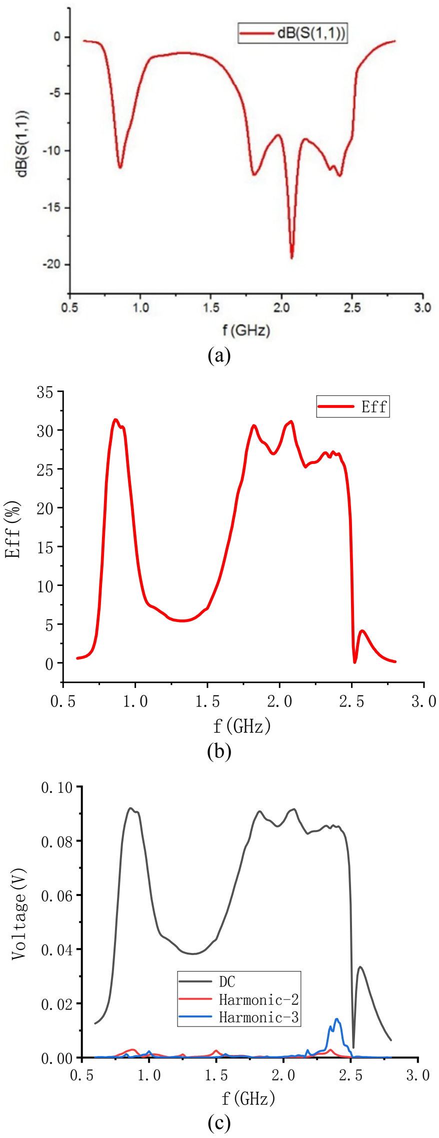

(a)

(b)

(c)

Fig. 11. (a) The reflection coefficient of rectifier. (b) Rectifying efficiency. (c) DC output voltage and harmonic components of the resulting DC output voltage.

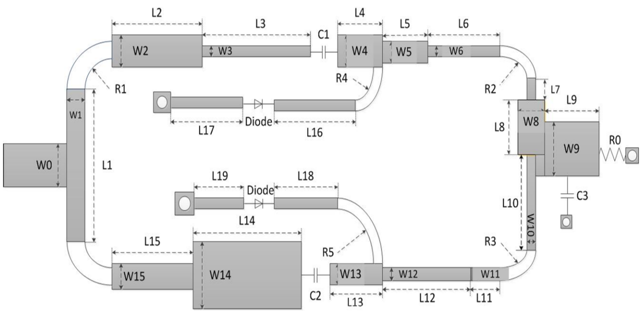

Fig. 12. The layout structure of rectifier.

W0	W1	L1	W2	L2	W3	L3	W4	L4
10	4.8	12	6	26.6	1.2	33	2.5	5.6
W5	**L5**	**W6**	**L6**	**L7**	**W8**	**L8**	**W9**	L9
2	4.1	1.1	4.7	4	5.3	8.5	5	9.4
W10	**L10**	**W11**	**L11**	**W12**	**L12**	**W13**	**L13**	**W14**
0.2	12.2	0.2	1.3	0.3	6.9	0.6	4.2	9.4
L14	**W15**	**L15**	**L16**	**L17**	**L18**	**L19**	**R1**	**R2**
36	4.6	24.1	27.6	24.1	6	13.9	5.9	1.5
R3	**R4**	**R5**	**R0**	**C1**	**C2**			
3	10.6	3.9	2700Ω	560 pF	530 pF			

Tab. 4. The physical parameter of rectifier (unit: mm).

Combining with the above two rectifiers, a novel topological structure of rectifier is presented in Fig. 10. To verify the structure, the rectifier is simulated and implemented on a 1.575 mm-thick Rogers RO5880 substrate which has a loss tangent of 0.0009 and relative dielectric constant ε_r of 2.2. The design results are given in Fig. 11, and Figure 12 displays the layout structure, the physical parameter is also presented in Tab. 4.

In Fig. 11, it is shown that when the input power is –20 dBm, the rectifier has a high rectifying efficiency about 30% which can cover four major bands of GSM 900 MHz, GSM 1800 MHz, UMTS 2100 MHz, WLAN 2400 MHz.

3. Measurement and Analysis

To verify the validity, the rectifier has been fabricated and tested as shown in Fig. 13 and Fig. 14, respectively. Before the test is done, it is necessary to solder the single SMS7630-079, GCM2165C2A561JA16 and GCM21A7U2E102JX01.

In Fig. 14, it is shown that when the input power is –20 dBm, the resonant frequency is offset, and the return loss and rectifying efficiency become worse clearly. It is due

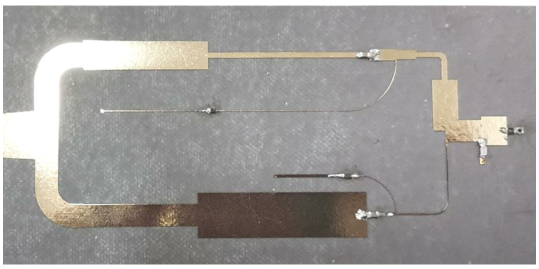

Fig. 13. The fabricated prototype.

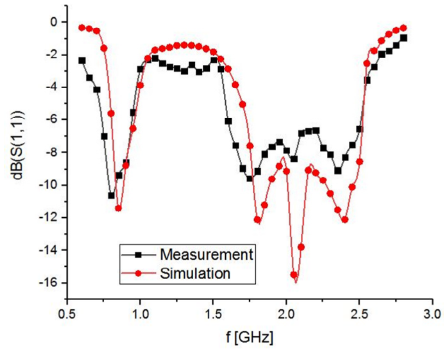

(a)

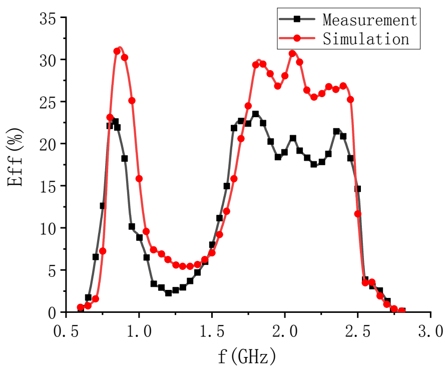

(b)

Fig. 14. (a) The reflection coefficient measurement. (b) The rectifying efficiency measurement.

to the package inductance of diode and the parasitic inductance of soldering electronic elements, which causes the resonant frequency to shift to low frequency. Similarly, the S parameter gets worse because of machining error, soldering SMA, the parasitic resistance of electronic components, which leads to the decline of rectifying efficiency. But it is acceptable in general and the measured efficiency can reach about 20% in four target bands.

4. Conclusion

In this letter, a high-sensitivity rectifying circuit is proposed which has higher efficiency in lower power level comparing with traditional voltage doubling circuit. To verify the idea, analysis and comparison are given by a design example, the results show that the improved circuit is better. At the same time, aiming at the target bands, this paper also designs a wideband impedance matching network. Combining with the proposed high-sensitivity rectifying circuit, a high-sensitivity broadband rectifier can be achieved. Comparing with previous works, the rectifier has higher rectifying efficiency under the same lower input power.

Acknowledgments

This work is supported by the Key Project of Natural Science Research in Anhui Universities in 2020

KJ2020A1189, and the National Nature Science Foundation of China 51477001.

References

[1] PINUELA, M., MITCHESON, P. D., LUCYSZYN, S. Ambient RF energy harvesting in urban and semi-urban environments. *IEEE Transactions on Microwave Theory and Techniques,* 2013, vol. 61, no. 7, p. 2715–2726. DOI: 10.1109/TMTT.2013.2262687

[2] TAVARES, J., BARROCA, N., SARAIVA, H. M., et al. Spectrum opportunities for electromagnetic energy harvesting from 350 MHz to 3 GHz. In *2013 7th International Symposium on Medical Information and Communication Technology (ISMICT).* Tokyo (Japan), 2013, p. 126–130. DOI: 10.1109/ISMICT.2013.6521714

[3] SONG, C., HUANG, Y., ZHOU, J., et al. A broadband efficient rectenna array for wireless energy harvesting. In *2015 9th European Conference on Antennas and Propagation (EuCAP).* Lisbon (Portugal), 2015, p. 1–5. ISSN: 2164-3342

[4] MANSOUR, M. M., KANAYA, H. Compact RF rectifier circuit for ambient energy harvesting. In *2017 IEEE International Symposium on Radio-Frequency Integration Technology (RFIT*). Seoul (South Korea), 2017, p. 220–222. DOI: 10.1109/RFIT.2017.8048256

[5] HUANG, Y., SHINOHARA, N., TOROMURA, H. A wideband rectenna for 2.4 GHz-band RF energy harvesting. In *2016 IEEE Wireless Power Transfer Conference (WPTC)*. Aveiro (Portugal), 2016, p. 1–3. DOI: 10.1109/WPT.2016.7498816

[6] OLGUN, U., CHEN, C. C., VOLAKIS, J. L. Low-profile planar rectenna for batteryless RFID sensors. In *2010 IEEE Antennas and Propagation Society International Symposium*. Toronto (Canada), 2010, p. 1–4. DOI: 10.1109/APS.2010.5562220

[7] REN, Y. J., CHANG, K. 5.8-GHz circularly polarized dual-diode rectenna and rectenna array for microwave power transmission. *IEEE Transactions on Microwave Theory and Techniques*, 2006, vol. 54, no. 4, p. 1495–1502. DOI: 10.1109/TMTT.2006.871362

[8] FARINHOLT, K. M., PARK, G., FARRAR, C. R. RF energy transmission for a low-power wireless impedance sensor node. *IEEE Sensors Journal,* 2009, vol. 9, no. 7, p. 793–800. DOI: 10.1109/JSEN.2009.2022536

[9] KHANSALEE, E., ZHAO, Y., LEELARASMEE, E., et al. A dual-band rectifier for RF energy harvesting systems. In *2014 11th International Conference on Electrical Engineering/Electronics, Computer, Telecommunications and Information Technology (ECTI-CON)*. Nakhon Ratchasima (Thailand), 2014, p. 1–4. DOI: 10.1109/ECTICon.2014.6839870

[10] KUHN, V., LAHUEC, C., SEGUIN, F., et al. A multi-band stacked RF energy harvester with RF-to-DC efficiency up to 84%. *IEEE Transactions on Microwave Theory and Techniques,* 2015, vol. 63, no. 5, p. 1768–1778. DOI: 10.1109/TMTT.2015.2416233

[11] VU, H. S., NGUYEN, N., HA-VAN, N., et al. Multiband ambient RF energy harvesting for autonomous IoT devices. *IEEE Microwave and Wireless Components Letters*, 2020, vol. 30, no. 12, p. 1189–1192. DOI: 10.1109/LMWC.2020.3029869

[12] TAFEKIRT, H., PELEGRI-SEBASTIA, J., BOUAJAJ, A., et al. A sensitive triple-band rectifier for energy harvesting applications. *IEEE Access,* 2020, vol. 8, p. 73659–73664. DOI: 10.1109/ACCESS.2020.2986797

[13] SONG, C., HUANG, Y., CARTER, P., et al. A novel six-band dual CP rectenna using improved impedance matching technique for ambient RF energy harvesting. *IEEE Transactions on Antennas and Propagation,* 2016, vol. 64, no. 7, p. 3160–3171. DOI: 10.1109/TAP.2016.2565697

[14] LIU, Z., ZHONG, Z., GUO, Y. X. Enhanced dual-band ambient RF energy harvesting with ultra-wide power range. *IEEE Microwave and Wireless Components Letters,* 2015, vol. 25, no. 9, p. 630–632. DOI: 10.1109/LMWC.2015.2451397

[15] MOULAY, A., DJERAFI, T. Multi-stage Schottky diode power harvester for UWB application. In *2018 IEEE Wireless Power Transfer Conference (WPTC)*. Montreal (QC, Canada), 2018, p. 115–119. DOI: 10.1109/WPT.2018.8639080

[16] SONG, C., HUANG, Y., ZHOU, J., et al. Improved ultrawideband rectennas using hybrid resistance compression technique. *IEEE Transactions on Antennas and Propagation,* 2017, vol. 65, no. 4, p. 2057–2062. DOI: 10.1109/TAP.2017.2670359

[17] LIU, W., HUANG, K., WANG, T., et al. A broadband high-efficiency RF rectifier for ambient RF energy harvesting. *IEEE Microwave and Wireless Components Letters*, 2020, vol. 30, no. 12, p. 1185–1188. DOI: 10.1109/LMWC.2020.3028607

[18] SONG, C., HUANG, Y., J. ZHOU, J., et al. A high-efficiency broadband rectenna for ambient wireless energy harvesting. *IEEE Transactions on Antennas and Propagation,* 2015, vol. 63, no. 8, p. 3486–3495. DOI: 10.1109/TAP.2015.2431719

[19] PALAZZI, V., HESTER, J., BITO, J., et al. A novel ultra-light-weight multiband rectenna on paper for RF energy harvesting in the next generation LTE bands. *IEEE Transactions on Microwave Theory and Techniques,* 2017, vol. 66, no. 1, p. 366–379. DOI: 10.1109/TMTT.2017.2721399

[20] WU, Y., LIU, Y., LI, S. A dual-frequency transformer for complex impedances with two unequal sections. *IEEE Microwave and Wireless Components Letters,* 2009, vol. 19, no. 2, p. 77–79. DOI: 10.1109/LMWC.2008.2011315

[21] CHOW, Y. L., WAN, K. L. A transformer of one-third wavelength in two sections - for a frequency and its first harmonic. *IEEE Microwave and Wireless Components Letters*, 2002, vol. 12, no. 1, p. 22–23. DOI: 10.1109/7260.975723

[22] MONZON, C. Analytical derivation of a two-section impedance transformer for a frequency and its first harmonic. *IEEE Microwave and Wireless Components Letters*, 2002, vol. 12, no. 10, p. 381–382. DOI: 10.1109/LMWC.2002.804558

[23] MONZON, C. A small dual-frequency transformer in two sections. *IEEE Transactions on Microwave Theory and Techniques*, 2003, vol. 51, no. 4, p. 1157–1161. DOI: 10.1109/TMTT.2003.809675

[24] MILLIGAN, T. A. Transmission-line transformation between arbitrary impedances (Letters). *IEEE Transactions on Microwave Theory and Techniques*, 1976, vol. 24, no. 3, p. 159–159. DOI: 10.1109/TMTT.1976.1128802

[25] POTOK, M. H. N. Comments on "Transmission-line transformation between arbitrary impedances" (Letters). *IEEE Transactions on Microwave Theory and Techniques*, 1977, vol. 25, no. 1, p. 77–77. DOI: 10.1109/TMTT.1977.1129040

[26] HUANG, L., LI, M., ZHANG, P., et al. A novel miniaturized UWB bandpass filter basing on E-shaped defected microstrip structure. *Progress In Electromagnetics Research Letters*, 2020, vol. 93, p. 49–57. DOI: 10.2528/PIERL20062601

About the Authors ...

Xuehua WANG (corresponding author) was born in Shandong, China. She received her M.Sc. from the University of Science and Technology of China in 2013. Her research interests include microwave circuits and devices, wireless transmission and antenna design.